Environmental Science & Technology

Article

Cite This: Environ. Sci. Technol. 2019, 53, 7355−7362

pubs.acs.org/est

Simultaneous and Synergic Production of Bioavailable Iron and Reactive Iodine Species in Ice

Kitae Kim,[†,‡,§] Sunil Paul M. Menacherry,[‡] Jungwon Kim,[∥] Hyun Young Chung,[§] Daun Jeong,[‡] Alfonso Saiz-Lopez,[⊥] and Wonyong Choi*[,‡]

[†]Korea Polar Research Institute (KOPRI), Incheon 21990, Korea

[‡]Division of Environmental Science and Engineering, Pohang University of Science and Technology (POSTECH), Pohang 37673, Korea

[§]Department of Polar Sciences, University of Science and Technology (UST), Incheon 21990, Korea

[∥]Department of Environmental Sciences and Biotechnology, Hallym University, Chuncheon, Gangwon-do 24252, Korea

[⊥]Department of Atmospheric Chemistry and Climate, Institute of Physical Chemistry Rocasolano, CSIC, Madrid 28006, Spain

Supporting Information

ABSTRACT: The bioavailable iron is essential for all living organisms, and the dissolution of iron oxide contained in dust and soil is one of the major sources of bioavailable iron in nature. Iodine in the polar atmosphere is related to ozone depletion, mercury oxidation, and cloud condensation nuclei formation. Here we show that the chemical reaction between iron oxides and iodide (I^-) is markedly accelerated to produce bioavailable iron ($Fe(II)_{aq}$) and tri-iodide (I_3^-: evaporable in the form of I_2) in frozen solution (both with and without light irradiation), while it is negligible in aqueous phase. The freeze-enhanced production of $Fe(II)_{aq}$ and tri-iodide is ascribed to the freeze concentration of iron oxides, iodides, and protons in the ice grain boundaries. The outdoor experiments carried out in midlatitude during a winter day (Pohang, Korea: 36°0′ N, 129°19′ E) and in an Antarctic environment (King George Island: 62°13′ S 58°47′ W) also showed the enhanced generation of $Fe(II)_{aq}$ and tri-iodide in ice. This study proposes a previously unknown abiotic mechanism and source of bioavailable iron and active iodine species in the polar environment. The pulse input of bioavailable iron and reactive iodine when ice melts may influence the oceanic primary production and CCN formation.

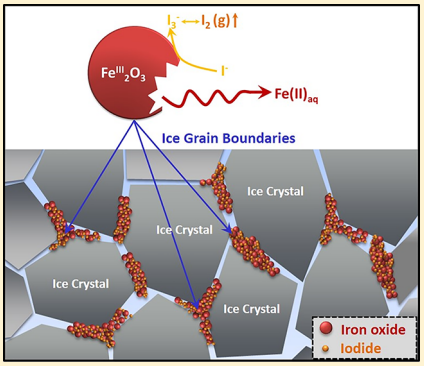

INTRODUCTION

Iron is an essential micronutrient for living organisms and plays an important role in various phytoplankton metabolisms.[1,2] In particular, oceanic primary productivity is limited by bioavailable iron (mainly ferrous species, Fe(II)) in several oceans including the Southern Ocean, which has low phytoplankton production despite the abundant nutrients (HNLC regions: high nutrient low chlorophyll).[3,4] Since the "iron hypothesis" was first proposed by Martin and co-workers,[3,5] various iron fertilization experiments ranging from incubation experiments to mesoscale iron enrichment experiments have been carried out. These experiments have revealed that the iron supply stimulates ocean primary production which is followed by atmospheric carbon sequestration through the biological carbon pump.[6,7] It is also known that one of the dominant iron sources to the open ocean is aeolian transport of dusts (containing iron) from the desert areas.[8] The speciation, solubility, and bioavailability of iron in the oceanic environment are controlled by chemical complexation with organic compounds and photochemical redox processes. The particulate iron (oxyhydr)oxides, which cannot be directly used by phytoplankton, can be transformed to bioavailable forms of iron through photochemical reactions in the ocean.[9] It has been also observed that the photochemical dissolution of iron oxides is enhanced in the presence of various organic compounds.[10]

The importance of iodine in the troposphere has been intensively studied due to its role in catalytic ozone depletion.[11] In addition to ozone destruction, iodine also plays important roles in (i) atmospheric oxidizing capacity by removing various organic and inorganic compounds,[12] (ii) generation of ultrafine aerosol particles as cloud condensation nuclei (CCN),[13] (iii) depletion of gaseous elemental mercury (Hg^0) via oxidation to Hg(II),[11] and (iv) perturbation of HO_x and NO_x ratio in midlatitudes marine boundary layer (MBL).[11,14] High concentrations (up to 20 pptv) of iodine oxide (IO) have been detected by ground- and satellite-based measurements in a coastal Antarctic region during spring time.[12] Furthermore, a remarkable 3-fold increase in Arctic atmospheric iodine levels has recently been reported for the period 1950−2011.[15] Although the environmental impacts of

Received: November 26, 2018
Revised: May 3, 2019
Accepted: May 13, 2019
Published: May 13, 2019

DOI: 10.1021/acs.est.8b06659
Environ. Sci. Technol. 2019, 53, 7355−7362

atmospheric iodine are subject to intensive research via field measurements, laboratory, and theoretical studies, the plausible production mechanisms of iodine in polar environment are still unclear.[16] Iodine is also suggested to be a potential proxy for past sea ice extent reconstructions.[17] However, the chemical transformation of iodine compounds during transport and after deposition on the ice media is not well-known. Understanding chemical transformation of iodine compounds in ice is essential to explain the relationship between iodine recorded in ice cores and paleo sea ice extent or glacial/interglacial variations.

It has been gradually revealed that ice and snow play a significant role as active media for environmental chemical processes such as photochemical, redox, and biological reactions.[18−24] The chemical processes involving organic and inorganic species in the frozen environment are thought to be quite different from their aqueous counterparts, and several reactions are significantly accelerated in the ice media. For example, the dissolution of metal oxide particles[19,25] and the reduction of Cr(VI) by organic acids[20]/H_2O_2[26]/NO_2^-[27] are highly enhanced in the frozen solutions. The photochemical (or dark) transformation of iodide ions to tri-iodide (I_3^-) and gaseous molecular iodine (I_2) is also highly enhanced in the ice phase.[28] It is generally thought that the accelerated chemical reactions in frozen solutions are caused by the freeze concentration effect in ice grain boundaries where organic or inorganic substrates are superconcentrated.[29]

Ice edge algal bloom during polar spring time has been observed and input of iron from melting sea ice is regarded as one of the major regulating factors.[30] Atmospheric mineral dusts containing iron oxide are transported and deposited on snow/ice layer on sea ice, and the concentration of iron in sea ice is much higher (up to several μM) relative to ice-free waters.[31] Furthermore, iodide exists in seawater at the concentration of tens to hundreds nM.[32] When seawater freezes, the iodide ions and biologically produced iodine species can be concentrated on the surface of sea ice. Considering that the dissolution of iron oxides in ice is sensitively affected by the presence and kind of various organic and inorganic species,[19,33,34] the reaction between iron oxides and iodide in ice may play an important role. Here we investigated the reductive dissolution of iron oxide to bioavailable iron ($Fe(II)_{aq}$) and the concurrent oxidation of iodide to reactive iodine species (I_3^-, I_2) in aqueous[35] and frozen solutions to reveal a previously unrecognized chemical transformation in the ice media.

MATERIALS AND METHODS

Materials. The synthesis and characterization of optically transparent α-Fe_2O_3 colloid are described in a previous paper.[19] Other commercially available iron oxides of hematite (α-Fe_2O_3, Bayferrox 105 M, LANXESS, BET surface area 6 m^2/g), maghemite (γ-Fe_2O_3, Aldrich, BET surface area 36 m^2/g), goethite (α-FeOOH, Aldrich, BET surface area 178 m^2/g), lepidocrocite (γ-FeOOH, Bayferrox 943, LANXESS, BET surface area 75 m^2/g), and magnetite (Fe_3O_4, Aldrich, BET surface area 50 m^2/g) were also used and compared with the colloidal hematite for the iron dissolution reactions. Arizona test dust (AZTD) containing 2−5% of Fe_2O_3 was employed as a proxy of natural mineral dust. Detailed information on AZTD can be found at www.powdertechnologyinc.com. Commercial iron oxide samples were ground into fine powder before preparing the stock aqueous suspension to enhance the dispersion. KI (99.5%, Samchun Chemical) was used as the iodide source. Argon gas (Linde Korea, 99.999% purity) was used as a purging gas when the dissolved O_2 was removed. Ultrapure deionized water (18 MΩ·cm) prepared by a Barnstead purification system was used in all experiments.

Photolysis. The detailed freezing and photolysis methods are described in our previous works.[19] To put it briefly, the samples containing colloidal hematite or various commercial iron oxides with iodide were placed in 12 × 125 mm quartz tubes, sealed with septa, and located in a merry-go-round photolysis reactor. The reactor was immersed into the cryogenic ethanol bath cooled at −5 °C. The temperature of cryogenic bath was gradually lowered to −20 °C within 20 min in order to prevent the breakage of the quartz tubes. A 100-W mercury lamp (Ace Glass Inc.) was used as a major UV irradiation source, and the lamp was placed in a double-jacket Pyrex well (cooled by ethanol circulation through the jacket) to prevent the direct contact between the lamp surface and the frozen solution. Irradiation wavelengths shorter than 300 nm were filtered by the Pyrex jacket surrounding the mercury lamp. After freeze solidification of the samples, the mercury lamp with Pyrex jacket was immersed in the cryogenic ethanol bath to start ice photochemical reaction. Aqueous photochemical reactions of iron oxides with iodide were also carried out as a control at 25 °C using the same experimental setup. For the photochemical experiments in deaerated condition, the sample tubes were purged with argon gas for 30 min prior to light irradiation. The light intensities absorbed by the aqueous and frozen samples were measured by the ferrioxalate actinometry method. Although the incident light flux from the mercury lamp should be the same, the intensities of the UV light absorbed by the aqueous and ice samples (λ > 300 nm) were 52.9 and 23.4 mW cm^{-2} (3.4×10^{-4} and 1.5×10^{-4} einstein min^{-1} L^{-1}), respectively. It should be noted that the light intensity absorbed by the frozen sample should be taken only as a rough estimate.[36] The measured value of light intensity in ice phase has some uncertainty because the ferrioxlate actinometry is mainly recommended for liquid phase.[37]

Dark Reaction. A conical centrifuge tube of 15 mL was used as a main reactor for the dark reactions. The samples containing colloidal hematite or commercial iron oxide with iodide were solidified in the cryogenic ethanol bath cooled at −20 °C. The aqueous samples were solidified within 20−30 min. Therefore, defining the time *zero* ("t = 0") in the reaction kinetic measurements was ambiguous. In this study, the time *zero* indicates the point when the aqueous sample was placed into the cryogenic ethanol bath precooled at the desired reaction temperature (−20 °C). Aqueous reactions of iron oxides with iodide were also carried out as a control at 25 °C using the same experimental setup. After reaction, the frozen samples were thawed usually within 5 min in a beaker containing lukewarm water (30−40 °C). All reactions were repeated at least three times to confirm the reproducibility.

Analysis. The concentration of $Fe(II)_{aq}$ was measured spectrophotometrically by using the ferrozine or 1,10-phenanthroline method,[19] and the total dissolved iron (Fe^{2+} and Fe^{3+}) was quantified by the same method following the chemical reduction of $Fe(III)_{aq}$ to $Fe(II)_{aq}$. We also measured the total dissolved iron (Fe^{2+} and Fe^{3+}) concentrations by atomic absorption spectroscopy (AAS, SpectrAA-800) to confirm that the above spectrophotometric method and the AA analysis attain the identical results. The concentration of

DOI: 10.1021/acs.est.8b06659
Environ. Sci. Technol. 2019, 53, 7355−7362

I_3^- was determined by measuring the absorbance at 352 nm (ε_m = 26,400 M^{-1} cm^{-1}) using a UV/visible spectrophotometer (Libra S22).

Outdoor Experiments. The outdoor experiments were carried out on the roof of the Environmental Engineering building at POSTECH (Pohang, Korea: 36°00′ N, 129°19′ E) between 9 a.m. and 2 p.m. under clear or partly cloudy sky conditions in January (winter season). The solar light intensity was recorded every minute by using a pyranometer (apogee, PYR-P), and a daily average varied from 20 to 51 mW cm^{-2}. The ambient temperature ranged between −3.7 and 1.9 °C. The same 12 × 125 mm quartz tubes that were used in the laboratory experiments were also used as a reactor for the outdoor experiments. Quartz tubes containing the desired concentrations of iron oxide and iodide were frozen in an ethanol bath before exposing to sunlight. The frozen samples are placed on the precooled ice pack to keep the samples from melting during the experiments. The control photolysis of aqueous samples was carried out simultaneously under the same irradiation conditions, and the aqueous samples were placed on an electrically heated mat to prevent the freezing of them. The concentrations of photogenerated $Fe(II)_{aq}$ and I_3^- were immediately determined by a UV/visible spectrophotometer after solar irradiation. We also carried out the same solar experiments in the Antarctic region, the King Sejong Station, King George Island (62°13′ S 58°47′ W, sea level) from December 15 to 24, 2013. The ambient temperature ranged between −5.5 and 1.7 °C (an average of −3.6 °C). The integrated solar irradiance measured at the King Sejong Station varied from 0.08 to 0.97 mW cm^{-2} for a UV band of 315 < λ < 380 nm. The quartz tubes containing desired concentrations of iron oxides and iodide in distilled water were frozen in a refrigerator cooled at −20 °C prior to natural solar irradiation. It took about 1 h for full solidification of samples.

RESULTS AND DISCUSSION

Enhanced Photochemical Production of $Fe(II)_{aq}$ and Triiodide in Ice. We carried out a series of photoreactions of iron oxides and iodide with monitoring the photoreductive dissolution of $Fe(II)_{aq}$ from iron oxides and the accompanying oxidation of iodide to triiodide. The production of both $Fe(II)_{aq}$ and I_3^- was significantly accelerated in the ice phase while negligible in the aqueous solution (Figure 1a).

$$\alpha\text{-}Fe_2O_3 + 3I^- + 6H^+ \rightarrow 2Fe^{2+} + I_3^- + 3H_2O \quad (1)$$

Although hematite (α-Fe_2O_3) can be reductively dissolved under extremely high concentrations of iodide and protons at high temperature (353 K)[38] in aqueous solution (eq 1), the reaction was negligible in the present aqueous condition (lower concentrations of proton, iron, and iodide, lower temperature). The reaction was apparently accelerated in the frozen solution with producing Fe^{2+} and I_3^- at a 2:1 molar ratio, which is close to the eq 1 stoichiometry. Incidentally, the possible photodissolution of Fe^{3+} species from hematite was checked by comparing the total dissolved iron concentration ($[Fe^{2+}]$ + $[Fe^{3+}]$) with $[Fe(II)_{aq}]$: most dissolved iron was Fe^{2+}, and the production of Fe^{3+} species was negligible. Therefore, the dissolved iron species is a result of reductive dissolution of iron oxide. Figure 1b shows that $Fe(II)_{aq}$ production in ice gradually increased with increasing the concentration of iodide. As for the pH effect, the photoreductive production of $Fe(II)_{aq}$ in both aqueous solution and ice was higher at lower pH value[10] (SI Figure S1a) which is in accord with eq 1. $Fe(II)_{aq}$ formation was insignificant above pH 5. On the other hand, I_3^- formation via photooxidation of iodide was also faster with lower pH but slightly reduced at pH 2 (Figure S1b). Unlike the case of $Fe(II)_{aq}$ formation, the photooxidative formation of I_3^- was still observed above pH 5, which reconfirms the recent study of photooxidation of iodide in ice.[28] It is well-known that I_3^- has equilibrium with I_2 in the presence of I^- ($I_2 + I^- \leftrightarrow I_3^-$: K = 700), and the detection of I_3^- implies the presence of I_2. The chemical equilibrium for the hydration of pyruvic acid was also observed in frozen state.[39] The spontaneous conversion of I_3^- to I_2 in frozen solution and the subsequent evaporation of I_2 to the gas phase over the ice were detected by cavity ring-down spectroscopy (CRDS).[28] We also monitored the possible production of oxyanions such as IO_3^- and IO_4^- that can be generated from the oxidation of I^- using ion chromatography, but no generation of such oxyanions (within their detection limit of about 0.5 μM) was observed.

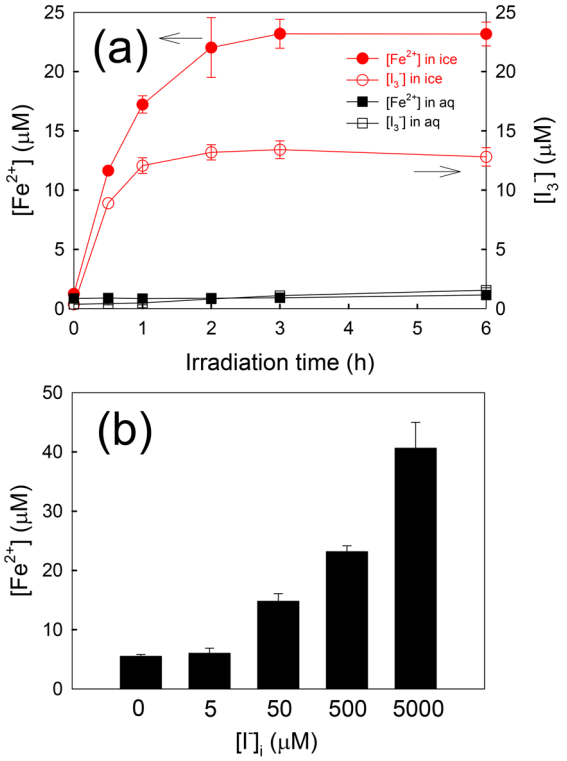

Figure 1. (a) Time profile of the simultaneous generation of $Fe(II)_{aq}$ and I_3^- in the UV-irradiated (λ > 300 nm) colloidal solution of hematite and I^- in aqueous phase (at 25 °C) or in ice (at −20 °C). (b) Production of $Fe(II)_{aq}$ from photoreductive dissolution of hematite with different concentrations of iodide contained in ice at −20 °C (after 6 h reaction). Experimental conditions: [α-Fe_2O_3] = 8 mg/L, $[I^-]_i$ = 500 μM (for a), pH_i = 3.

To evaluate the role of dioxygen, the photoreactions of hematite and iodide were compared between aerated and deaerated conditions (SI Figure S2). The production of Fe(II) was enhanced in ice both with and without dissolved O_2. The $Fe(II)_{aq}$ formation via photodissolution of hematite should be hindered in the aerated condition since dioxygen can reoxidize the reduced $Fe(II)_{surf}$ or scavenge the conduction band electrons in iron oxide particles.[40] However, it is interesting to note that the inhibiting effect of O_2 on the hematite photodissolution was much lower in ice than that in the

DOI: 10.1021/acs.est.8b06659
Environ. Sci. Technol. 2019, 53, 7355−7362

aqueous phase. This implies that the iron dissolution reaction (eq 1) is strongly favored with concentrated reagents (e.g., I^-) in the ice grain boundary, and the hindering effect of O_2 is much limited in ice compared with that in the aqueous solution. On the contrary, the concurrent photooxidation of iodide to I_3^- was highly accelerated in the presence of O_2 in both aqueous solution and ice since iodide can be directly oxidized by O_2 (eq 2).[28]

$$O_2(aq) + 4H^+ + 6I^- \rightarrow 2H_2O + 2I_3^- \quad (2)$$

The photooxidation of iodide to triiodide is negligible in the absence of O_2 in both aqueous and frozen solutions containing the iodide only.[28] However, the present result shows that this anoxic mechanism of iodide photooxidation is enabled in the presence of hematite (SI Figure S2b). This implies that the photoactivation of iodide is possible even in O_2-free (or O_2-deficient) environmental conditions as long as iron oxide is available.

Enhanced Production of $Fe(II)_{aq}$ and Triiodide under Dark Conditions. The reaction of hematite and iodide was also tested in the absence of light. Figure 2 shows that the dark

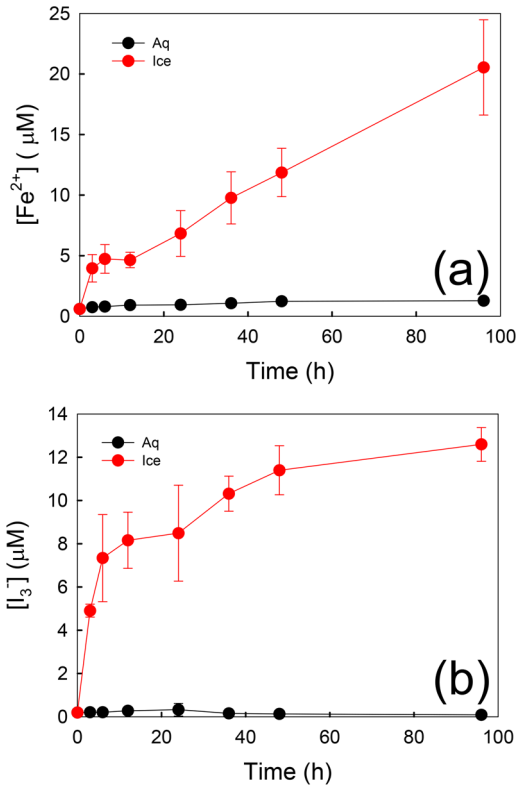

Figure 2. Time profiles of the simultaneous generation of (a) $Fe(II)_{aq}$ and (b) I_3^- in the colloidal solution of hematite and I^- in aqueous phase (at 25 °C) or in ice (at −20 °C) in the dark. Experimental conditions: [α-Fe_2O_3] = 8 mg/L, $[I^-]_i$ = 500 μM, pH_i = 3.

redox reaction induced a significant production of $Fe(II)_{aq}$ and I_3^- in the ice phase (though much slower than the photochemical counterpart shown in Figure 1a), while that in aqueous solution was negligible. The final molar ratio of [$Fe(II)_{aq}$] and [I_3^-] after 96 h reaction was close to the stoichiometric ratio of 2:1 as in the case of a photochemical reaction (see Figure 1a).

The simultaneous redox conversion of iron oxide and iodide in ice under dark conditions was also tested using various types of iron oxides (commercially available powder) which have different characteristics such as particle size, surface area, and crystallinity [hematite (α-Fe_2O_3), maghemite (γ-Fe_2O_3), goethite (α-FeOOH), lepidocrocite (γ-FeOOH), and magnetite (Fe_3O_4)]. The results are summarized in Table 1. The

Table 1. Formation of $Fe(II)_{aq}$ via Reductive Dissolution of Various Types of Iron Oxides and Simultaneous Production of I_3^- from I^- Oxidation under Dark Conditions[a]

	[$Fe(II)_{aq}$] (μM)		[I_3^-] (μM)	
	aq	ice	aq	ice
hematite (α-Fe_2O_3)	1.1 ± 0.6	4.8 ± 1.2	0.1	7.8 ± 0.8
maghemite (γ-Fe_2O_3)	3.3 ± 0.4	169.1 ± 3.4	0.1	26.8 ± 1.4
goethite (α-FeOOH)	8.1 ± 1.2	101.1 ± 2.2	0.6 ± 0.3	22.4 ± 0.9
lepidocrocite (γ-FeOOH)	0.9 ± 0.4	148.4 ± 3.7	0.1	31.6 ± 1.6
magnetite (Fe_3O_4)	2.5 ± 0.5	218.7 ± 5.5	0.2	30.9 ± 2.1

[a]Experimental conditions: [iron oxide] = 0.2 g/L, [I^-] = 1 mM, pH_i = 3, reaction time 72 h in aqueous solution at 25 °C and in ice at −20 °C.

production of $Fe(II)_{aq}$ and I_3^- under the dark was markedly enhanced in the ice phase regardless of the kind of iron oxides. We also investigated the pH dependence of $Fe(II)_{aq}$ and I_3^- production under dark conditions (SI Figure S3). The formation of both $Fe(II)_{aq}$ and I_3^- was enhanced in ice phase and decreased with increasing pH. The generation of $Fe(II)_{aq}$ was negligible above pH 5 even in ice phase. This trend is coincident with the previous finding.[33]

Comparison with the Single Component Freezing Systems. We compared the production of $Fe(II)_{aq}$ or I_3^- in ice between the single component (γ-Fe_2O_3 or iodide only) and the dual (γ-Fe_2O_3 + iodide) components systems (SI Table S1). The production of $Fe(II)_{aq}$ from iron oxide in ice was significantly accelerated in the presence of iodide (the dual components) compared to the case of iron oxide only (the single component) in both dark and irradiated conditions. UV irradiation enhanced the reductive dissolution rate of γ-Fe_2O_3 by iodide in ice about 12 times (initial dissolution rates under dark and UV irradiation are 3.75 μM/h and 45 μM/h, respectively) compared to that under dark conditions. However, it seems that the iodide oxidation was not apparently enhanced by the presence of γ-Fe_2O_3 in ice. This implies that triiodide ions are adsorbed or further decomposed back to iodide on γ-Fe_2O_3. The photochemical oxidation of iodide in ice was also accelerated both in the presence and absence of iron oxide.

Freeze Concentration Effect and Reaction Mechanism. Accelerated chemical reactions in ice are mainly attributed to the freeze concentration effect of reagents in ice grain boundaries.[29,41,42] To investigate this concentration effect on this photoredox reaction (hematite + iodide) in ice, the aqueous phase reaction was carried out with higher concentrations of iodide and proton. The reference reaction was carried out with [I^-] = 0.5 mM and pH 3 in both aqueous and frozen solutions, which proceeded only in the ice phase (Figure 3). When either the concentration of [I^-] or [H^+] in aqueous solution was raised by 10-fold (from the reference reaction), the production of $Fe(II)_{aq}$ was also observed in

DOI: 10.1021/acs.est.8b06659
Environ. Sci. Technol. 2019, 53, 7355−7362

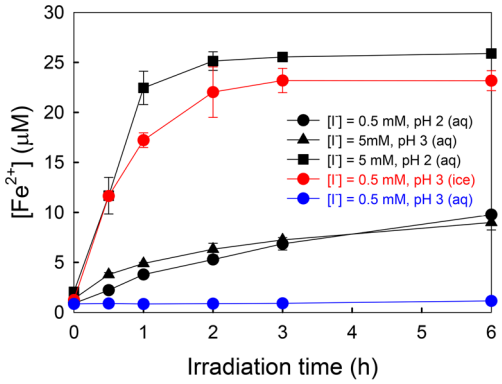

Figure 3. Effect of $[I^-]$ and pH on $Fe(II)_{aq}$ generation via the photoreductive dissolution of hematite (8 mg/L) in aqueous solutions (at 25 °C) in comparison with the reference ice phase reaction performed with $[I^-]$ = 0.5 mM and pH 3 (red circles).

aqueous solution although it was still much lower than that in the ice reference reaction. However, when both $[I^-]$ and $[H^+]$ were raised by 10 times ($[I^-]$ = 5 mM, pH 2), the production of Fe(II) in aqueous solution was comparable to or even higher than that in the ice reference reaction. This implies that the enhanced reaction of hematite and iodide in ice can be ascribed to the concentration of reagents in the ice grain boundary.

The reductive dissolution of hematite by iodide was previously investigated under extreme conditions (i.e., pH 2, high concentrations of iodide (0.5−1.56 M), and high temperature (353 K)) to propose the following rate law (eq 3):[37] the first order with respect to proton concentration and the second order with respect to the concentration of iodide.

$$R = k[H^+][I^-]^2 \quad (3)$$

The redox conversion of iron oxide and iodide should require the surface adsorption (or complexation) of iodide on the Fe_2O_3 surface. To verify the adsorption (or complexation) of I^- on the Fe_2O_3 surface, the attenuated total reflection Fourier transform infrared (ATR-FTIR) spectra of pure Fe_2O_3 and I^--adsorbed Fe_2O_3 were measured and compared (SI Figure S4). I^- adsorbed on Fe site in Fe_2O_3 can inhibit the vibration of Fe−O vibration. The peak at 560 cm^{-1}, which is ascribed to Fe−O vibration,[43] was significantly reduced by I^- adsorption. This result indicates that the adsorption (or complexation) of I^- on the surface of Fe_2O_3 is favored. The adsorption (or complexation) of I^- on the Fe_2O_3 surface can be enabled by electrostatic attraction between I^- and the OH_2^+ group on Fe_2O_3 (outer-sphere surface complex) or ligand exchange between I^- and the OH (or OH_2^+) group on Fe_2O_3 (inner-sphere surface complex).[37] Figure S5 shows a high-resolution transmission electron microscopy (HRTEM) image, an energy-dispersive X-ray (EDX) spectrum, and elemental mapping images of I^--adsorbed Fe_2O_3. The I peak in the EDX spectrum reconfirms that I^- can be adsorbed on the surface of Fe_2O_3. I elemental spots are well scattered and exactly coincide the Fe and O elemental spots.

The adsorption of I^- on the Fe_2O_3 surface could be followed by the electron transfer from the adsorbed iodide to the iron oxide through two mechanisms: (1) the ligand-to-metal charge transfer (LMCT) from adsorbed iodide to the surface ferric ion or (2) the photoinduced charge transfer on hematite working as a photocatalyst. From a LMCT viewpoint, ferric ion on the hematite surface (noted as ≡Fe(III)) forms an inner-sphere complex with the adsorbed iodide (eq 4), and the subsequent LMCT reduces ferric to ferrous species with oxidizing iodide (eqs 5 and 6). It was previously reported that the interfacial process can be highly facilitated in the ice grain boundary region where the concentrations of iron oxide particles and organic/inorganic molecules/ions are highly elevated.[19,33,34] The resulting iodide radical reacts with another iodide anion to produce diiodine radical ($E^0(I_2/I_2^{\bullet -})$ = 0.11 V) (eq 7), which seems to explain why the overall reaction rate law is the second order with respect to the concentration of iodide (eq 3). The reduced surface Fe(II) is then dissolved into the solution (eq 8), and the diiodine radicals disproportionate to produce triiodide (eq 9).

$$\equiv Fe(III) + I^- \rightarrow \equiv Fe(III)\text{-}I^- \quad \text{(inner-sphere surface complex)} \quad (4)$$

$$\equiv Fe(III)\text{-}I^- \rightarrow \equiv Fe(II)\text{-}I\cdot \quad \text{(LMCT)} \quad (5)$$

$$\equiv Fe(III)\text{-}I^- + h\nu \rightarrow \equiv Fe(II)\text{-}I\cdot \quad \text{(photoinduced LMCT)} \quad (6)$$

$$\equiv Fe(II)\text{-}I\cdot + I^- \rightarrow \equiv Fe(II) + I_2^{\bullet -} \quad (I^- \text{ reaction}) \quad (7)$$

$$Fe(II)_{surf}\ \text{(surface site)} \rightarrow \mathbf{Fe(II)_{aq}} \quad \text{(desorption)} \quad (8)$$

$$I_2^{\bullet -} + I_2^{\bullet -} \rightarrow \mathbf{I_3^-} + I^- \ \text{(disproportionation)} \quad (9)$$

An alternative mechanism is the semiconductor photocatalysis where the reductive dissolution of $Fe(II)_{aq}$ and the oxidation of iodide are caused by the photoinduced transfers of conduction band (CB) electron and valence band (VB) hole, respectively, on hematite semiconductor (E_g = 2.2 eV) (eqs 10−13). The photogenerated CB electrons can reduce lattice Fe(III) to Fe(II) (eq 11) which is subsequently released into the solution phase (eq 12). On the other hand, iodide is oxidized to I_3^- by VB holes (eq 13).

$$Fe^{III}{}_2O_3 + h\nu \rightarrow e_{cb}^- + h_{vb}^+ \quad \text{(bandgap excitation)} \quad (10)$$

$$Fe(III)\ (\textit{surface site}) + e_{cb}^- \rightarrow Fe(II)_{surf}\ \text{(iron reduction)} \quad (11)$$

$$Fe(II)_{surf}\ (\textit{surface site}) \rightarrow \mathbf{Fe(II)_{aq}}\ \text{(desorption)} \quad (12)$$

$$\equiv Fe(III)\text{-}I^- + h_{vb}^+ \rightarrow \equiv Fe(III)\text{-}I\cdot$$

$$\equiv Fe(III)\text{-}I\cdot + I^- \rightarrow \equiv Fe(III) + I_2^{\bullet -}\ \text{(iodide oxidation)} \quad (13)$$

The redox reaction between ferric ions and iodide ions is thermodynamically spontaneous (eq 14),[44] and therefore the dark reaction can occur without photoactivation.

$$2Fe^{3+} + 3I^- \rightarrow 2Fe^{2+} + I_3^- \quad E^0 = 1.01\ V_{NHE} \quad (14)$$

Accordingly, the stoichiometric molar ratio of Fe^{2+} and I_3^- production reached 2:1 in the photostationary state (see Figure 1a). However, in the initial reaction period (<1 h), the relative concentration of photogenerated $Fe(II)_{aq}$ with respect to I_3^- is significantly lower than the ratio of 2:1. This could be ascribed to the slow dissolution process of $Fe(II)_{surf}$ from the iron oxide surface (eq 8).

Solar Experiments. To confirm the applicability to natural solar irradiation, outdoor experiments were conducted under natural environmental conditions in midlatitude during a

DOI: 10.1021/acs.est.8b06659
Environ. Sci. Technol. 2019, 53, 7355−7362

winter day (Pohang, Korea: 36°00′ N, 129°19′ E) (Figure 4). The simultaneous generation of $Fe(II)_{aq}$ and I_3^- was

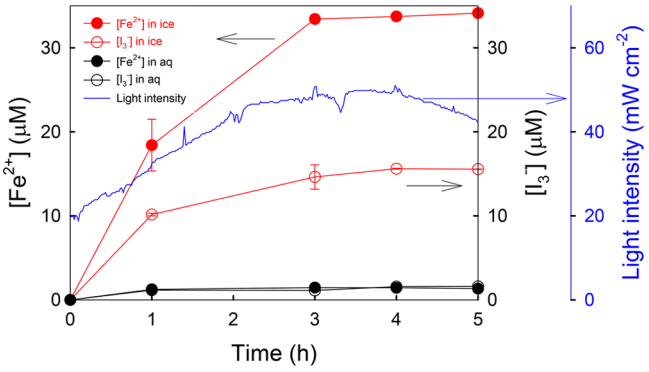

Figure 4. Simultaneous production of $Fe(II)_{aq}$ and I_3^- in the natural solar-irradiated solution of hematite and I^- in aqueous phase (at 25 °C) or in ice (at −20 °C). Experimental conditions: [α-Fe_2O_3] = 8 mg/L (50 μM), [I^-] = 500 μM, pH_i = 3.

concurrently accelerated in ice under solar irradiation. The production of $Fe(II)_{aq}$ and I_3^- under solar irradiation conditions was slightly higher than that in laboratory conditions using an artificial light source (100 W medium pressure Hg lamp) (see the Methods section). We also carried out the solar experiments in an Antarctic environment at King George Island (62°13′ S 58°47′ W, sea level) (see Figure 5).

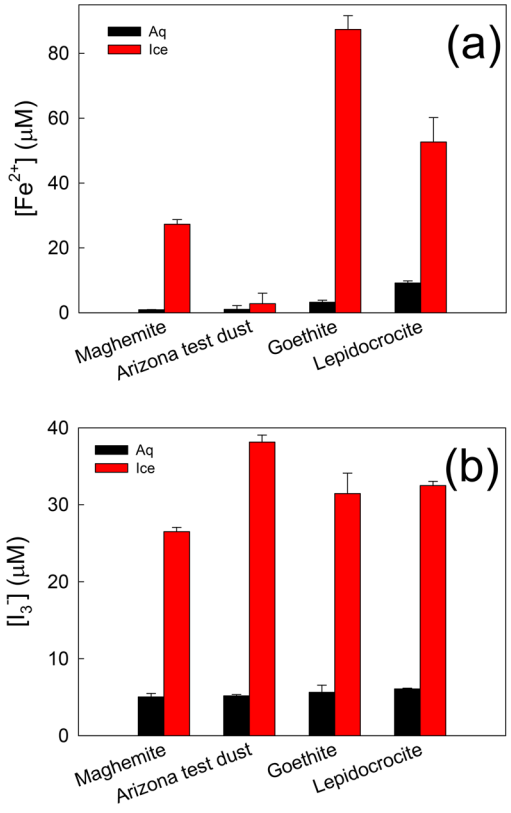

Figure 5. Simultaneous production of (a) $Fe(II)_{aq}$ and (b) I_3^- in the solution of iron oxide and I^- in aqueous phase (at 25 °C) or in ice (at −20 °C) under solar irradiation in an Antarctic region (King George Island, 62°13′ N, 58°47′ E). Experimental conditions: [iron oxide or Arizona test dust] = 0.2 g/L, [I^-] = 1 mM, pH_i = 3, 7 h irradiation.

The production of $Fe(II)_{aq}$ and I_3^- in ice was consistently higher than that in the aqueous phase regardless of the kind of iron oxides. Figure 5 compared the production of $Fe(II)_{aq}$ and I_3^- from various iron oxide samples (maghemite, goethite, and lepidocrocite: the properties summarized in Table S2) after 7 h of reaction under Antarctic solar irradiation. The production of $Fe(II)_{aq}$ in ice phase was most closely related with the surface area of the iron oxide sample, while other properties of iron oxide such as the surface potential and hydrodynamic diameter seem to have little correlation with the photoactivity. Goethite has the highest surface area (178 m^2/g) and exhibited the highest production of $Fe(II)_{aq}$ (87.4 ± 3.0 μM) after 7 h in ice phase. Maghemite which has the lowest surface area (36 m^2/g) produced the smallest amount of dissolved Fe(II) (27.3 ± 1.0 μM) in ice. Lepidocrocite with a medium surface area (75 m^2/g) showed the medium reactivity (52.7 ± 5.3 μM). Arizona test dust which contained 2−5% of Fe_2O_3 also exhibited an enhanced production of $Fe(II)_{aq}$ in ice phase compared to aqueous solution. The production of $Fe(II)_{aq}$ should depend on the surface area of iron oxide because the ferrous species are dissolved from the surface sites (eqs 8 and 12). On the other hand, the production of triiodide was much less influenced by the type of iron oxides in both aqueous and ice phase (Figure 5b), which is consistent with the observation that the iodide oxidation was not apparently enhanced by the presence of γ-Fe_2O_3 in ice (Table S1). The production of triiodide seems to be little influenced by the iron oxide part. The outdoor experiments confirm that the photoreaction of iron oxide and iodide can be accelerated in frozen solutions not only in the laboratory conditions but also under natural solar irradiation.

Environmental Implications. The reductive dissolution of iron oxides and the accompanying oxidation of iodide to I_3^- were compared between the aqueous and ice phases. The redox transformation that produces bioavailable $Fe(II)_{aq}$ and reactive iodine species (I_3^- then I_2) proceeded negligibly slowly in aqueous solution but was significantly accelerated in frozen solution both under light irradiation and in the dark. The frozen solution contains iodides, protons, and iron oxide particles concentrated in ice grain boundaries, which should accelerate the heterogeneous reactions. The freeze-enhanced redox reaction of iron oxide and iodide might occur in natural environments. Although the present experimental finding is unlikely applicable to seawater conditions because of the high pH of seawater (between 7.5 and 8.4), atmospheric dust particles containing iron can travel a long distance and can be trapped in ice aerosols containing sea salts. The pH of aerosols can be decreased to pH 1−2 in the presence of organic and inorganic acids. Acidic aerosols containing iron mineral dusts[45] and frozen sea salt aerosols containing iodide are commonly found in cold environments (atmosphere in polar regions, the upper troposphere and stratosphere).[46] In addition, snow/ice on frozen sea may contain iron species provided through the atmospheric transport and deposition of mineral dusts and iodide supplied by wind-driven seawater droplets. It is also reported that an acid rock drainage and rock weathering site in Antarctica provides acidic (pH 3.2−4.5) and iron-rich (up to 1.78 mM Fe) drainage water into the ocean. They also measured the concentration of dissolved iron in sea ice (1.9 μM−29 μM), which is comparable to our study (50 μM as total iron).[47] The present work suggests that the intrinsic chemical reactions occurring in the ice phase can have important environmental implications and therefore need to

DOI: 10.1021/acs.est.8b06659
Environ. Sci. Technol. 2019, 53, 7355−7362

be further investigated from the microscopic to the global scale.

We suggest that the concomitant production of active iodine (I_3^-, I_2) along with iron reduction in ice may partly contribute to the abrupt increase of atmospheric iodine concentrations in the Antarctic spring.[12,44] This has implications for CCN formation and radiative forcing[48] as reported in previous research connecting atmospheric iodine and particle formation in both the Arctic and Antarctic atmospheres.[49]

The supply of bioavailable iron plays a critical role in biogeochemical processes such as enhancement of primary production in HNLC regions. This work suggests that particulate iron oxides present in polar aerosols, snow, sea ice, icebergs, and ice sheets may be quickly converted into the bioavailable form of iron ($Fe(II)_{aq}$) through (photo)reductive dissolution processes. The previously observed high concentration of bioavailable iron and algal bloom near receding ice might be partially explained by the enhanced reduction of iron oxides trapped in ice.[30] The synergically enhanced production of bioavailable iron and active iodine species through the frozen-media transformation path might play a significant role in the global environmental processes.

■ ASSOCIATED CONTENT

Supporting Information

The Supporting Information is available free of charge on the ACS Publications website at DOI: 10.1021/acs.est.8b06659.

pH effect, photoreductive production of $Fe(II)_{aq}$ in both aqueous solution and ice, Figure S1; photoreactions of hematite and iodide compared between aerated and deaerated conditions, Figure S2; pH dependence of $Fe(II)_{aq}$ and I_3^- production under dark conditions, Figure S3; ATR-FTIR spectra of pure Fe_2O_3 and I^--adsorbed Fe_2O_3 measured and compared, Figure S4; HRTEM image, EDX spectrum, and elemental mapping images of I^--adsorbed Fe_2O_3, Figure S5; compared production of $Fe(II)_{aq}$ or I_3^- in ice between single component and dual component systems, Table S1; maghemite, goethite, and lepidocrocite: properties summarized, Table S2 (PDF)

■ AUTHOR INFORMATION

Corresponding Author

*E-mail: wchoi@postech.edu.

ORCID

Kitae Kim: 0000-0003-0803-3547
Sunil Paul M. Menacherry: 0000-0002-9487-9874
Jungwon Kim: 0000-0001-7804-7587
Daun Jeong: 0000-0001-7703-5226
Alfonso Saiz-Lopez: 0000-0002-0060-1581
Wonyong Choi: 0000-0003-1801-9386

Notes

The authors declare no competing financial interest.

■ ACKNOWLEDGMENTS

Funding for this work was provided by Korea Polar Research Institute (KOPRI) project (PE19200).

■ REFERENCES

(1) Morel, F. M. M.; Price, N. M. The biogeochemical cycles of trace metals in the oceans. *Science* **2003**, *300*, 944−947.

(2) Turner, D. R.; Hunter, K. A. *The biogeochemistry of iron in seawater*, 7th ed.; John Wiley & Sons, Ltd.: Chichester, 2001.

(3) Martin, J. H.; Gordon, R. M.; Fitzwater, S. E. Iron in Antarctic waters. *Nature* **1990**, *345*, 156−159.

(4) Hopwood, M. Iron from ice. *Nat. Geosci.* **2018**, *11*, 462−462.

(5) Martin, J. H. Glacial-Interglacial CO_2 change: the iron hypothesis. *Paleoceanography* **1990**, *5*, 1−13.

(6) Boyd, P. W.; Watson, A. J.; Law, C. S.; Abraham, E. R.; Trull, T.; Murdoch, R.; Bakker, D. C. E.; Bowie, A. R.; Buesseler, K. O.; Chang, H.; Charette, M.; Croot, P.; Downing, K.; Frew, R.; Gall, M.; Hadfield, M.; Hall, J.; Harvey, M.; Jameson, G.; Liddicoat, J. L.; Ling, R.; Maldonado, M. T.; McKay, R. M.; Nodder, S.; Pickmere, S.; Pridmore, R.; Rintoul, S.; Safi, K.; Sutton, P.; Strzepek, R.; Tanneberger, K.; Turner, S.; Waite, A.; Zeldis, J. A mesoscale phytoplankton bloom in the polar Southern Ocean stimulated by iron fertilization. *Nature* **2000**, *407*, 695−702.

(7) Chisholm, S. W. Stirring times in the Southern Ocean. *Nature* **2000**, *407*, 685−686.

(8) Jickells, T. D.; An, Z. S.; Andersen, K. K.; Baker, A. R.; Bergametti, G.; Brooks, N.; Cao, J. J. Global iron connection between desert dust, ocean biogeochemistry, and climate. *Science* **2005**, *308*, 67−71.

(9) Finden, D. A. S.; Tipping, E.; Jaworski, G. H. M.; Reynolds, C. S. Light-induced reduction of natural iron(III) oxide and its relevance to phytoplankton. *Nature* **1984**, *309*, 783−784.

(10) Pehkonen, S. O.; Siefert, R.; Erel, Y.; Webb, S.; Hoffmann, M. R. Photoreduction of iron oxyhydroxides in the presence of important atmospheric organic compounds. *Environ. Sci. Technol.* **1993**, *27*, 2056−2062.

(11) Saiz-Lopez, A.; Plane, J. M. C.; Mahajan, A. S.; Anderson, P. S.; Bauguitte, S. J.-B.; Jones, A. E.; Roscoe, H. K.; Salmon, R. A.; Bloss, W. J.; Lee, J. D.; Heard, D. E. On the vertical distribution of boundary layer halogens over coastal Antarctica: implications for O_3, HO_x, NO_x and the Hg lifetime. *Atmos. Chem. Phys.* **2008**, *8*, 887−900.

(12) Saiz-Lopez, A.; Mahajan, A. S.; Salmon, R. A.; Bauguitte, S. J.-B.; Jones, A. E.; Roscoe, H. K.; Plane, J. M. C. Boundary layer halogens in coastal Antarctica. *Science* **2007**, *317*, 348−351.

(13) Hoffmann, T.; O'Dowd, C. D.; Seinfeld, J. H. Iodine oxide homogeneous nucleation: An explanation for coastal new particle production. *Geophys. Res. Lett.* **2001**, *28*, 1949−1952.

(14) Bloss, W. J.; Lee, J. D.; Johnson, G. P.; Sommariva, R.; Heard, D. E.; Saiz-Lopez, A.; McFiggans, G.; Coe, H.; Flynn, M.; Williams, P.; Rickard, A. R.; Fleming, Z. L. Impact of halogen monoxide chemistry upon boundary layer OH and HO_2 concentrations at a coastal site. *Geophys. Res. Lett.* **2005**, *32*, L06814.

(15) Cuevas, C. A.; Maffezzoli, N.; Corella, J. P.; Spolaor, A.; Vallelonga, P.; Kjaer, H. A.; Simonsen, M.; Winstrup, M.; Vinther, B.; Horvat, C.; Fernandez, R. P.; Kinnison, D.; Lamarque, J. F.; Barbante, C.; Saiz-Lopez, A. Rapid increase in atmospheric iodine levels in the North Atlantic since the mid-20th century. *Nat. Commun.* **2018**, *9*, 1452.

(16) Saiz-Lopez, A.; Blaszczak-Boxe, C. S. The polar iodine paradox. *Atmos. Environ.* **2016**, *145*, 72−73.

(17) Spolaor, A.; Vallelonga, P.; Plane, J. M. C.; Kehrwald, N.; Gabrieli, J.; Varin, C.; Turetta, C.; Cozzi, G.; Kumar, R.; Boutron, C.; Barbante, C. Halogen species record Antarctic sea ice extent over glacial-interglacial periods. *Atmos. Chem. Phys.* **2013**, *13*, 6623−6635.

(18) Amoroso, A.; Domine, F.; Esposito, G.; Morin, S.; Savarino, J.; Nardino, M.; Montagnoli, M.; Bonneville, J.-M.; Clement, J.-C.; Ianniello, A.; Beine, H. J. Microorganisms in dry polar snow are involved in the exchanges of reactive nitrogen species with the atmosphere. *Environ. Sci. Technol.* **2010**, *44*, 714−719.

(19) Kim, K.; Choi, W.; Hoffmann, M. R.; Yoon, H.-I.; Park, B.-K. Photoreductive dissolution of iron oxides trapped in ice and its environmental implications. *Environ. Sci. Technol.* **2010**, *44*, 4142−4148.

(20) Kim, K.; Choi, W. Enhanced redox conversion of chromate and arsenite in ice. *Environ. Sci. Technol.* **2011**, *45*, 2202−2208.

DOI: 10.1021/acs.est.8b06659
Environ. Sci. Technol. 2019, 53, 7355−7362

(21) Dubowski, Y.; Hoffmann, M. R. Photochemical transformations in ice: Implications for the fate of chemical species. *Geophy. Res. Lett.* **2000**, *27*, 3321−3324.
(22) Dubowski, Y.; Colussi, A. J.; Boxe, C.; Hoffmann, M. R. Monotonic increase of nitrite yields in the photolysis of nitrate in ice and water between 238 and 294 K. *J. Phys. Chem. A* **2002**, *106*, 6967−6971.
(23) Guzman, M. I.; Hoffmann, M. R.; Colussi, A. J. Photolysis of pyruvic acid in ice: Possible relevance to CO and CO_2 ice core record anomalies. *J. Geophys. Res.* **2007**, *112*, D10123.
(24) Cheng, J.; Soetjipto, C.; Hoffmann, M. R.; Colussi, A. J. Confocal fluorescence microscopy of the morphology and composition of interstitial fluids in freezing electrolyte solutions. *J. Phys. Chem. Lett.* **2010**, *1*, 374−378.
(25) Kim, K.; Yoon, H. I.; Choi, W. Enhanced dissolution of manganese oxide in ice compared to aqueous phase under illuminated and dark conditions. *Environ. Sci. Technol.* **2012**, *46*, 13160−13166.
(26) Kim, K.; Kim, J.; Bokare, A. D.; Choi, W.; Yoon, H. I.; Kim, J. Enhanced removal of hexavalent chromium in the presence of H_2O_2 in frozen aqueous solutions. *Environ. Sci. Technol.* **2015**, *49*, 10937−10944.
(27) Kim, K.; Chung, H. Y.; Ju, J.; Kim, J. Freezing-enhanced reduction of chromate by nitrite. *Sci. Total Environ.* **2017**, *590*, 107−113.
(28) Kim, K.; Yabushita, A.; Okumura, M.; Saiz-Lopez, A.; Cuevas, C. A.; Blaszczak-Boxe, C. S.; Min, D. W.; Yoon, H. I.; Choi, W. Production of molecular iodine and tri-iodide in the frozen solution of iodide: Implication for polar atmosphere. *Environ. Sci. Technol.* **2016**, *50*, 1280−1287.
(29) Takenaka, N.; Ueda, A.; Maeda, Y. Acceleration of the rate of nitrite oxidation by freezing in aqueous solution. *Nature* **1992**, *358*, 736−738.
(30) Sedwick, P. N.; DiTullio, G. R. Regulation of algal blooms in Antarctic shelf water by the release of iron from melting sea ice waters. *Geophys. Res. Lett.* **1997**, *24*, 2515−2518.
(31) Lannuzel, D.; Vancoppenolle, M.; van der Merwe, P.; de Jong, J.; Meiners, K. M.; Grotti, M.; Nishioka, J.; Schoemann, V. Iron in sea ice: Review and new insights. *Elem. Sci. Anth.* **2016**, *4*, 000130.
(32) Atkinson, H. M.; Huang, R. J.; Chance, R.; Roscoe, H. K.; Hughes, C.; Davison, B.; Schonhardt, A.; Mahajan, A. S.; Saiz-Lopez, A.; Hoffmann, T.; Liss, P. S. Iodine emissions from the sea ice of the Weddell Sea. *Atmos. Chem. Phys.* **2012**, *12*, 11229−11244.
(33) Jeong, D.; Kim, K.; Min, D. W.; Choi, W. Freezing-enhanced dissolution of iron oxides: Effects of inorganic acid anions. *Environ. Sci. Technol.* **2015**, *49*, 12816−12822.
(34) Menacherry, S. P. M.; Kim, K.; Lee, W.; Choi, C. H.; Choi, W. Ligand-specific dissolution of iron oxides in frozen solutions. *Environ. Sci. Technol.* **2018**, *52*, 13766−13773.
(35) Pillar, E. A.; Guzman, M. I.; Rodriguez, J. M. Conversion of iodide to hypoiodous acid and iodine in aqueous microdroplets exposed to ozone. *Environ. Sci. Technol.* **2013**, *47*, 10971−10979.
(36) Hatchard, C. G.; Parker, C. A. A new sensitive chemical actinometer. II. Potassium ferrioxalate as a standard chemical actinometer. *Proc. R. Soc. London A* **1956**, *235*, 518−536.
(37) Kuhn, H. J.; Braslavsky, S. E.; Schmidt, R. Chemical Actonometry (IUPAC Technical Report). *Pure Appl. Chem.* **2004**, *76*, 2105−2146.
(38) Ali, S. P.; Blesa, M. A.; Morando, P. J.; Regazzoni, A. E. Reductive dissolution of hematite in acidic iodide solutions. *Langmuir* **1996**, *12*, 4934−4939.
(39) Guzman, M. I.; Hildebrandt, L.; Colussi, A. J.; Hoffmann, M. R. Cooperative hydration of pyruvic acid in ice. *J. Am. Chem. Soc.* **2006**, *128*, 10621−10624.
(40) Sulzberger, B.; Laubscher, H. Reactivity of various types of iron(hydr)oxides toward light-induced dissolution. *Mar. Chem.* **1995**, *50*, 103−115.
(41) Takenaka, N.; Ueda, A.; Daimon, T.; Bandow, H.; Dohmaru, T.; Maeda, Y. Acceleration mechanism of chemical reaction by freezing: The reaction of nitrous acid with dissolved oxygen. *J. Phys. Chem.* **1996**, *100*, 13874−13884.
(42) Grannas, A. M.; Bausch, A. R.; Mahanna, K. M. Enhanced aqueous photochemical reaction rates after freezing. *J. Phys. Chem. A* **2007**, *111*, 11043−11049.
(43) Namduri, H.; Nasrazadani, S. Quantitative analysis of iron oxides using Fourier transform infrared spectrophotometry. *Corros. Sci.* **2008**, *50*, 2493−2497.
(44) Laurence, G. S.; Ellis, K. J. Oxidation of iodide ion by iron(III) ion in aqueous solution. *J. Chem. Soc., Dalton Trans.* **1972**, *0*, 2229−2233.
(45) Fu, H.; Cwiertny, D. M.; Carmichael, G. R.; Scherer, M. M.; Grassian, V. H. Photoreductive dissolution of Fe-containing mineral dust particles in acidic media. *J. Geophys. Res.* **2010**, *115*, D11304.
(46) Saiz-Lopez, A.; Plane, J. M. C.; Baker, A. R.; Carpenter, L. J.; Glasow, R. V.; Martín, J. C. G.; McFiggans, G.; Saunders, R. W. Atmospheric Chemistry of Iodine. *Chem. Rev.* **2012**, *112*, 1773−1804.
(47) Dold, B.; González-Toril, E.; Aguilera, A.; Lopez, E.; Cisternas, M. E.; Bucchi, F.; Amils, R. Acid rock drainage and rock weathering in Antarctica: Important sources for iron cycling in the Southern Ocean. *Environ. Sci. Technol.* **2013**, *47*, 6129−6136.
(48) Roscoe, H. K.; Jones, A. E.; Brough, N.; Weller, R.; Saiz-Lopez, A.; Mahajan, A. S.; Schoenhardt, A.; Burrows, J. P.; Fleming, Z. L. Particles and iodine compounds in coastal Antarctica. *J. Geophys. Res. Atmos.* **2015**, *120*, 7144−7156.
(49) Sipila, M.; Sarnela, N.; Jokinen, T.; Henschel, H.; Junninen, H.; Kontkanen, J.; Richters, S.; Kangasluoma, J.; Franchin, A.; Perakyla, O.; Rissanen, M. P.; Ehn, M.; Vehkamaki, H.; Kurten, T.; Berndt, T.; Petaja, T.; Worsnop, D.; Ceburnis, D.; Kerminen, V. M.; Kulmala, M.; O'Dowd, C. Molecular-scale evidence of aerosol particle formation via sequential addition of HIO_3. *Nature* **2016**, *537*, 532−534.

DOI: 10.1021/acs.est.8b06659
Environ. Sci. Technol. 2019, 53, 7355−7362